Untangling the Effect of Head Acceleration on Brain Responses to Blast Waves

Haojie Mao
Department of Defense,
Biotechnology High Performance Computing
Software Applications Institute,
Telemedicine and Advanced Technology Research Center,
U.S. Army Medical Research and Materiel Command,
Fort Detrick, MD 21702

Ginu Unnikrishnan
Department of Defense,
Biotechnology High Performance Computing
Software Applications Institute,
Telemedicine and Advanced Technology Research Center,
U.S. Army Medical Research and Materiel Command,
Fort Detrick, MD 21702

Vineet Rakesh
Department of Defense,
Biotechnology High Performance Computing
Software Applications Institute,
Telemedicine and Advanced Technology Research Center,
U.S. Army Medical Research and Materiel Command,
Fort Detrick, MD 21702

Jaques Reifman[1]
Department of Defense,
Biotechnology High Performance Computing
Software Applications Institute,
Telemedicine and Advanced Technology Research Center,
U.S. Army Medical Research and Materiel Command,
504 Scott Street,
Fort Detrick, MD 21702
e-mail: jaques.reifman.civ@mail.mil

Multiple injury-causing mechanisms, such as wave propagation, skull flexure, cavitation, and head acceleration, have been proposed to explain blast-induced traumatic brain injury (bTBI). An accurate, quantitative description of the individual contribution of each of these mechanisms may be necessary to develop preventive strategies against bTBI. However, to date, despite numerous experimental and computational studies of bTBI, this question remains elusive. In this study, using a two-dimensional (2D) rat head model, we quantified the contribution of head acceleration to the biomechanical response of brain tissues when exposed to blast waves in a shock tube. We compared brain pressure at the coup, middle, and contre-coup regions between a 2D rat head model capable of simulating all mechanisms (i.e., the all-effects model) and an acceleration-only model. From our simulations, we determined that head acceleration contributed 36–45% of the maximum brain pressure at the coup region, had a negligible effect on the pressure at the middle region, and was responsible for the low pressure at the contre-coup region. Our findings also demonstrate that the current practice of measuring rat brain pressures close to the center of the brain would record only two-thirds of the maximum pressure observed at the coup region. Therefore, to accurately capture the effects of acceleration in experiments, we recommend placing a pressure sensor near the coup region, especially when investigating the acceleration mechanism using different experimental setups. [DOI: 10.1115/1.4031765]

Keywords: blast-induced traumatic brain injury, head acceleration, brain pressure, finite-element model

1 Introduction

Exposure to improvised explosive devices has been the main cause of "blast injuries" in U.S. Service Members deployed to Iraq and Afghanistan [1–4]. Blast exposures can cause a wide spectrum of injuries to the brain, ranging from mild primary injury to the more severe secondary and tertiary injuries. While the primary injury is attributed to the interaction of the blast wave with the brain (i.e., the blast overpressure (BOP), which may create regions of high pressure within the brain), the secondary and tertiary injuries are associated with penetrating and blunt trauma to the head, respectively, due to shrapnel and movement of the body [5–7].

Damage to brain tissues from BOP is suspected to be caused by (1) high-pressure differentials from stress-wave propagation within and through the skull (wave propagation) [8], (2) dynamic deformation of the skull (skull flexure) [9], or (3) bubble formation and subsequent collapse due to changes in pressure (cavitation effects) [10,11]. In addition to these widely accepted mechanisms, brain tissue damage can also be caused by rapid acceleration of the head resulting from the interaction of the blast wave with the head [12,13]. In fact, experimental studies have reported extremely high head acceleration, often in the range of 3500–37,500 m/s^2, in animals exposed to blast waves [12,13]. Goldstein et al. observed that mice with head restraints had significantly less brain tissue damage when compared to those without head restraints [14]. Similarly, Gullotti et al. reported that head acceleration can influence immediate neurological impairments in mice [12]. The observed high acceleration and the lower tissue damage in animals with head restraints both demonstrate the need to evaluate head acceleration as a potential bTBI mechanism. Moreover, an accurate quantitative characterization of the acceleration mechanism may be necessary for development of protective strategies against bTBI [15]. However, even though numerous blast-related experimental and computational animal studies have been performed [9,10,14,16–20], the specific contribution of the acceleration mechanism to bTBI remains elusive.

Biomechanical responses, such as pressure, stress, and strain, are correlated to brain tissue damage [21,22], and they provide valuable information on the response of brain tissue to external mechanical loading, such as BOP. Our objective was to perform computational investigations on the interaction of a blast wave with an animal head and, from the biomechanical responses of the brain, determine the contribution of head acceleration to bTBI. To this end, we developed a 2D computational rat head model and performed blast simulations in a shock tube. We then compared the pressure between the head model that captured all the mechanisms (i.e., an all-effects model) and an acceleration-only model. We also investigated the response of the brain tissues to the different orientations of the blast wave. The results of this study allowed us to uniquely quantify the contribution of the acceleration effects to the biomechanical responses of rat brain tissues.

2 Methods

We coupled a 2D rat head model developed from magnetic resonance imaging (MRI) scans with a 2D shock tube model to characterize the effects of blast waves on rat brain tissues. Using

[1]Corresponding author.
Manuscript received May 8, 2015; final manuscript received September 21, 2015; published online October 30, 2015. Assoc. Editor: Barclay Morrison.

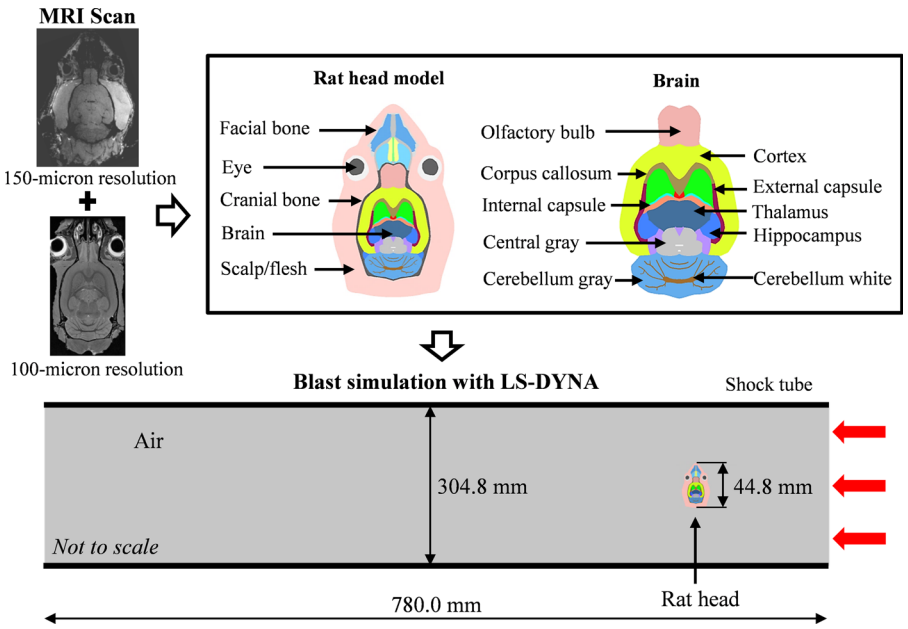

Fig. 1 Description of the computational blast simulation. We developed the 2D rat head model based on MRI data from the Duke University (anatomical features of the skull and brain at 100 μm resolution) [23] and the University of Utah (anatomical features of the scalp/flesh and facial bones at 150 μm resolution) [24]. We used LS-DYNA (Livermore Software Technology Corporation, Livermore, CA) to perform the shock tube blast simulations.

the coupled rat head and shock tube models, we performed simulations at various BOPs and blast wave orientations.

2.1 Rat Head Model

2.1.1 Geometry. We created the 2D rat head model by combining an axial MRI slice of the head of a 250 g male Wistar rat [23] and of a 400 g male Wistar rat [24]. The MRI slice from the 250 g rat had a higher resolution (100 μm) with a more detailed brain anatomy than the MRI from the 400 g rat (150 μm); however, it did not have the complete scalp and facial components (Fig. 1). From the 100 μm resolution MRI slice, we identified the major brain components, such as the olfactory bulb, cortex, corpus callosum, external capsule, internal capsule, hippocampus, thalamus, central gray, cerebellum gray, and cerebellum white. For the complete scalp and facial components, we used the 150 μm resolution image from the 400 g rat. We obtained this image from the University of Utah's imaging facility [24], where researchers used a 7-T Bruker Biospec MRI scanner (Bruker Biospin, Inc., Ettlingen, Germany) interfaced with a 12 cm, actively shielded gradient insert capable of producing a magnetic field gradient up to 600 mT/m. They used a 50-mm inner diameter quadrature radio-frequency coil (Rapid Biomedical, Rimpar, Germany) for MR signal transmission and reception, and a three-dimensional (3D) fast low-angle shot pulse sequence to obtain a complete coverage of the head with 25 ms repetition time, 5 ms echo time, 30 deg flip angle, and 25 averages.

We digitized the MRI axial slices using IMAGEJ 1.48v (National Institutes of Health, Bethesda, MD) and imported them into HYPERMESH 12.0 (Altair, Inc., Troy, MI). Using the existing relationships between brain and body weight [25], we scaled up the 100 μm resolution image by a factor of 1.009 and scaled down the 150 μ resolution image by a factor of 0.990 to develop a consolidated geometric model for a 300 g Wistar rat head.

2.1.2 Finite-Element (FE) Mesh. Deviatoric (stress/strain) responses in a solid are sensitive to mesh sizes. The recommended mesh size of hexahedral Lagrangian elements for an FE simulation of a blunt impact with a rat head should be less than 0.20 mm [26]. In this study, we used an average mesh size of 0.15 mm, which led to the creation of 23,836 hexahedral elements. We used a penalty function to define the brain–skull interface, omitting the thin layer of the cerebrospinal fluid, which is also excluded in a previously reported 3D rat head model [27]. We believe that the exclusion of the cerebrospinal fluid layer would not affect the FE predictions of brain pressure because the bulk moduli of the cerebrospinal fluid and the brain are the same (2.2 GPa).

2.1.3 Material Properties. We selected the material properties for the FE model from a previous bTBI simulation of a rat head [27]. We defined the elastic modulus of the skull as 9.5 GPa based on the blunt-impact-related experiments [28] and based on the volumetric responses of the brain tissue, skull, and scalp on linear elasticity, which describes the volumetric response associated with a bulk modulus. We used the same bulk modulus for the rat brain model as was used in a previous bTBI simulation [27]. We used linear viscoelastic materials for the rat brain model. Table 1 lists the material properties.

2.2 Shock Tube Model

2.2.1 Geometry. We simulated a rectangular shock tube with a width of 304.8 mm (1 ft) and length of 780.0 mm. The width was 6.8 times the length of our rat head (Fig. 1). We selected this width based on a parametric comparative study that simulated a shock tube with a width of 609.6 mm. We found that the pressures at the coup, middle, and contre-coup regions of the brain were very close for both cases, with differences of less than 0.1%.

2.2.2 FE Mesh. Volumetric response (i.e., pressure) in the brain is sensitive to air mesh sizes. We performed parametric studies using air mesh densities at 0.5, 1, 2, 4, and 8 mm. We found that an air mesh density of 2 mm offered acceptable accuracy, with peak brain pressures in the coup, middle, and contre-coup regions of the brain being less than 3% lower from those predicted by the air meshes with a 1 mm density.

2.2.3 Material Properties. The shock tube consisted of air, which we modeled as an ideal gas ($\gamma = 1.4$) with an initial pressure of 101.3 kPa and an initial density of 1.28 kg/m^3. We simulated the air dynamics using a second-order van Leer advection scheme

Table 1 Rat head material properties

Components	Properties
Olfactory bulb, cortex, hippocampus, thalamus, central gray, and cerebellum gray	$\rho = 1060\,\text{kg/m}^3$ $K = 2.2$ GPa $G_0 = 1.73$ kPa $G_\infty = 0.53$ kPa Decay constant $= 50\,\text{s}^{-1}$
Corpus callosum, internal capsule, external capsule, and cerebellum white	$\rho = 1060\,\text{kg/m}^3$ $K = 2.2$ GPa $G_0 = 2.08$ kPa $G_\infty = 0.64$ kPa Decay constant $= 50\,\text{s}^{-1}$
Scalp/flesh	$\rho = 1100\,\text{kg/m}^3$ $K = 2.2$ GPa $G_0 = 1.7$ MPa $G_\infty = 0.68$ MPa Decay constant $= 0.03\,\text{s}^{-1}$
Cranial bone	$\rho = 1500\,\text{kg/m}^3$ $E = 9.5$ GPa Poisson's ratio $= 0.35$
Facial bone	$\rho = 1500\,\text{kg/m}^3$ $E = 6.0$ GPa Poisson's ratio $= 0.35$
Eye	$\rho = 1006\,\text{kg/m}^3$ $E = 1.0$ MPa Poisson's ratio $= 0.4999$
Sinus	$\rho = 100\,\text{kg/m}^3$ $E = 1.0$ kPa Poisson's ratio $= 0.20$

Note: E, Young's modulus; G_0, short-term shear modulus; G_∞, long-term shear modulus; K, bulk modulus; and ρ, density.

available in LS-DYNA (Livermore Software Technology Corporation, Livermore, CA).

2.2.4 Boundary Condition. Similar to the model proposed by Sundaramurthy et al. [29], we simulated a partial shock tube. We prescribed Friedlander waveform incident pressures of 1-ms duration at the inlet and used a nonreflecting boundary condition at the open-end of the shock tube to allow air to exit. The air nodes in the upper and lower boundaries were constrained to simulate the walls of the shock tube.

2.3 Blast Simulation. We simulated blasts with LS-DYNA, using its fluid–structure interaction algorithm to couple the air domain and the rat head model. Similar methods have been used in the literature to simulate the interaction between blast waves and the head (e.g., see Refs. [27] and [30]).

2.3.1 All-Effects Model. The rat head model described in Sec. 2.1 included the combined effect of wave propagation, skull flexure, and acceleration mechanisms. In addition, to represent cavitation, we allowed the brain–skull interface to separate at a predefined negative pressure of 100 kPa.

2.3.2 Acceleration-Only Model. We evaluated the brain responses due to head acceleration by performing simulations using an acceleration-only rat head model. To implement such a model, we prescribed the cranial bone (Fig. 1) as a rigid material and we turned off the cavitation effects. The rigid cranial bone, while blocking the effects of wave propagation and flexure in the skull, did not affect head acceleration due to blast waves. An alternative approach to investigate the effect of acceleration would involve applying acceleration at the neck and using a deformable skull. However, it is possible that the brain response could be affected by the skull flexure, especially near the head–neck junction, preventing the isolation of the acceleration effect on the brain response.

2.3.3 Angle of Orientation and BOPs. We simulated three head orientations: lateral, frontal, and 45-deg angled (Fig. 2), with an incident BOP of 100 kPa. We further performed simulations at BOPs of 70 kPa and 130 kPa in the lateral orientation to investigate how different intensities of blast waves affect the brain response.

3 Results

We characterized the effect of head acceleration on brain responses due to blast waves and analyzed brain responses under various head orientations and BOPs.

In the all-effects model, we observed the highest brain pressure values at the coup region (Fig. 3(*a*)) and the lowest peak brain pressure values at the contre-coup region. After 0.2 ms following the initial increase, the pressures at the coup, middle, and contre-coup regions converged (Fig. 3(*a*)). As expected, initially, we observed high-pressure at coup region (Fig. 3(*b*), $t = 0.23$ ms); the high-pressure area quickly expanded and moved toward the contre-coup region (Fig. 3(*b*), $t = 0.24$ ms). The brain pressures decreased to lower magnitudes after the blast front passed through the head (Fig. 3(*b*), $t = 0.32$ ms).

In the acceleration-only model, we observed positive pressure at the coup region and negative pressure at the contre-coup region (Fig. 4(*a*)), which is a classical coup and contre-coup pressure distribution pattern generally observed under impact-loading conditions [31–34].

The brain pressure at the coup region from the acceleration-only head model was 36.6% of the pressure from the all-effects model (Fig. 4(*b*)). The pressure at the contre-coup region from the acceleration-only model was −83.7% of the pressure from the all-effects model (Fig. 4(*b*)). The acceleration-only model predicted nearly zero pressure at the middle region, while the all-effects model predicted a pressure of 131.9 kPa.

Head orientation affected wave dynamics, with the frontal position inducing larger areas of pressure reflections, and the 45-deg angled position directing the majority of the reflection to one side of the head (Fig. 5(*a*)). Such changes of wave dynamics, in

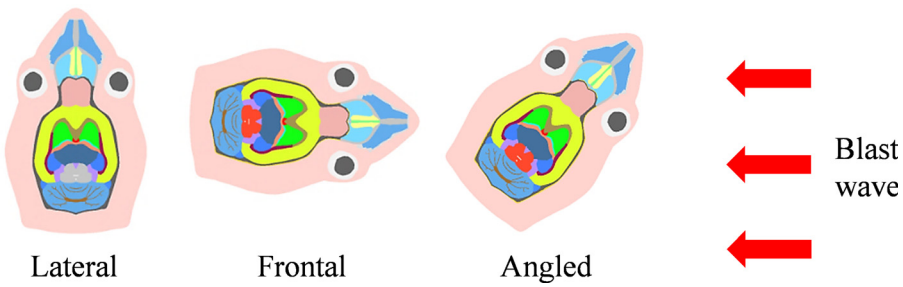

Fig. 2 Study design. We investigated the effects of head orientation by simulating lateral, frontal, and 45-deg angled impacts for both the all-effects and acceleration-only rat head models.

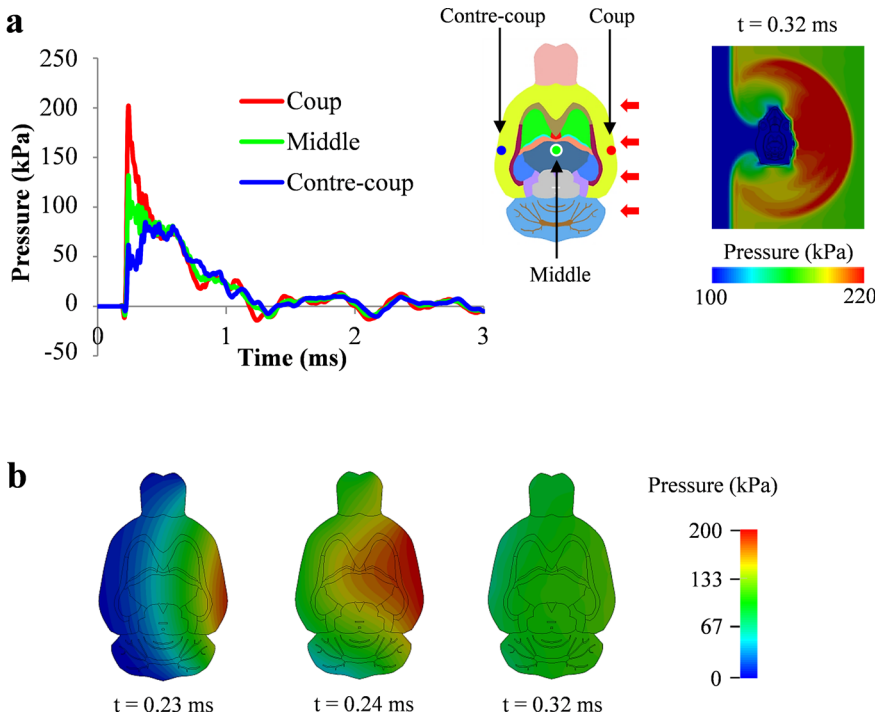

Fig. 3 Temporal and spatial distributions of brain pressure in the all-effects model. (*a*) Time histories of brain pressure at the coup, middle, and contre-coup regions for lateral impacts. The three time histories were different in the first 0.20 ms after the initial pressure increase, but rapidly converged. (*b*) Blast-wave-induced spatial distributions of brain pressure at three time points.

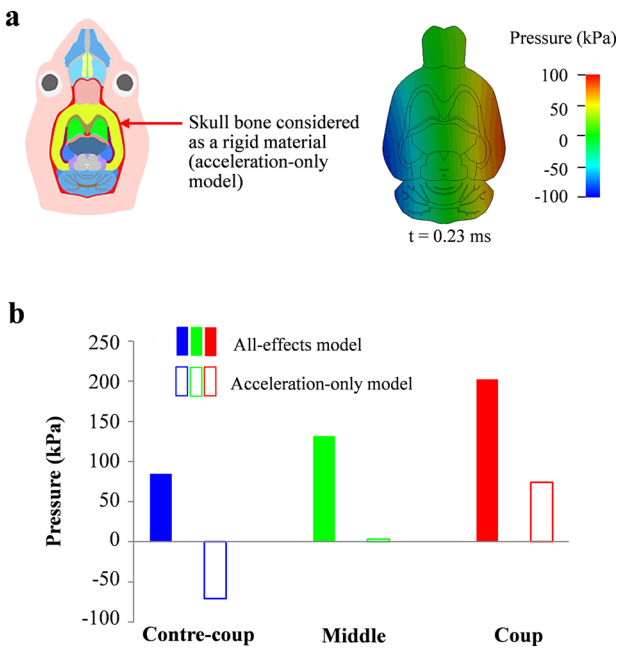

Fig. 4 Effect of blast-wave-induced head acceleration on brain pressure. (*a*) Typical brain pressure distribution predicted by the acceleration-only model. Head acceleration caused a positive pressure at the coup region and a negative pressure at the contre-coup region. (*b*) The pressure predicted by the acceleration-only model was 36.6% of that predicted by the all-effects model, indicating a moderate additive effect (with respect to other injury mechanisms) on brain pressure. Head acceleration did not affect brain pressure in the middle region. The brain pressure predicted by the acceleration-only model was −83.7% of that predicted by the all-effects model, indicating a subtractive effect on brain pressure due to head acceleration.

combination with the anatomic features of the rat head, modified the magnitudes of the brain pressures (Fig. 5(*b*)). The brain pressures due to the frontal impact were the lowest, whereas the brain pressures due to the angled impact were somewhere between those in the lateral (highest) and frontal (lowest) cases. For the frontal impact, the coup pressure was 45.1 kPa and the contre-coup pressure was −56.0 kPa, corresponding to 38.2% and −80.9% of the pressures predicted by the all-effects model, respectively. For the angled impact, the coup pressure was 71.6 kPa and the contre-coup pressure was −64.4 kPa, corresponding to 44.8% and −89.3% of the values predicted by the all-effects model, respectively. It should be noted that the various blast impact orientations (lateral, frontal, and angled) only mildly (less than 9%) affected the contributions of the head acceleration effect.

Lateral blast impact simulations with various incident pressures (70, 100, and 130 kPa) demonstrated that the brain pressures changed linearly with the incident pressures (detailed data not shown). Consequently, the ratios between pressures predicted by the all-effects model and acceleration-only model were similar. At the coup region, the head-acceleration-induced brain pressures were 36–37% of those from the all-effects model. At the contre-coup region, the head-acceleration-induced brain pressures were −80% to −90% of those from the all-effects model.

We observed that the deviatoric response of brain tissue to a blast wave was very small. For all the cases simulated, the brain–skull relative motions were less than 0.10 mm, the brain tissue strains were less than 1%, and the von Mises stresses were less than 1.0 kPa.

The head acceleration values were in the range of 6429–12,662 m/s^2. These high accelerations occurred in the millisecond time scale, consistent with the computational study on the human head response due to blast waves [35]. Despite high head acceleration, the rat head moved a maximum of 1.83 mm laterally after 3 ms of a 100 kPa lateral BOP impact simulation. For this simulation, the speed of the rat head reached 0.56 m/s after 3 ms.

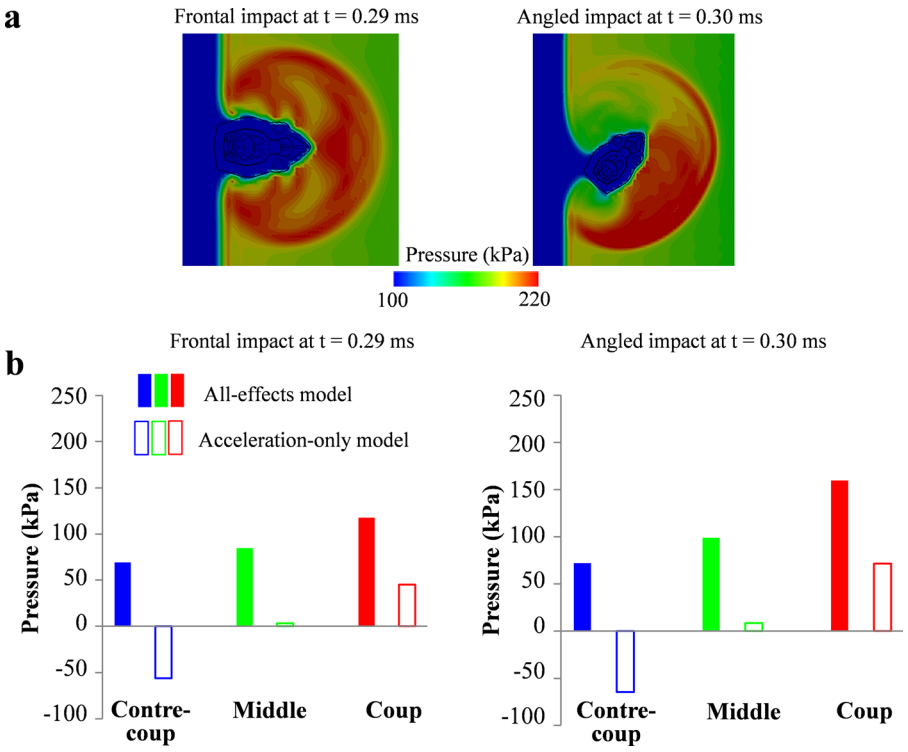

Fig. 5 Effect of head orientation on brain pressures. (*a*) Despite the difference in wave dynamics, (*b*) head orientations only modestly affected the contributions of head acceleration to brain pressure. For the frontal impact, the coup pressure predicted by the acceleration-only model was 38.2% of that predicted by the all-effects model. For the angled impact, this percentage was 44.8%. The contre-coup pressure predicted by the acceleration-only model was −80.9% of that predicted by the all-effects model for the frontal impact and −89.3% for the angled impact. For both the all-effects and acceleration-only models, the brain pressures in the frontal impact were the lowest, because of the energy absorption and wave divergence by facial components. The brain pressures in the 45-deg angled impact were between those of the lateral impact and the frontal impact.

4 Discussion

In this study, we developed a shock tube model and 2D computational rat head models (all-effects and acceleration-only) and quantitatively characterized the contribution of the acceleration mechanism on the biomechanical response of the rat brain when subjected to a BOP in a shock tube. The results from our simulations demonstrated that the head acceleration from blast exposure in a shock tube is an important mechanism affecting brain pressure. High brain pressures were previously reported to cause neuronal and vascular damage [36,37] and are often used as a metric for brain tissue damage. We determined that the head acceleration contributed over one third of the maximum brain pressure at the coup region, had no effect on the pressure at the middle region, and was responsible for the low pressure at the contre-coup region. We attribute this pressure distribution phenomenon to the highly accelerated rat skull that interacts with the brain, causing compression of the brain tissues at the coup region and tension at the contre-coup region.

These findings provide important guidance when performing bTBI experiments on small animals. Measurements of brain pressures were previously performed at locations close to the middle of the brain [14,29,38,39]. From the simulations performed in this study, we infer that head acceleration will not contribute to pressure in the center of the brain and, therefore, pressure sensors in the center of the brain will record only two-thirds of the maximum pressure observed at the coup region in the rat. Hence, we recommend placing the pressure sensor near the coup region, especially when investigating the acceleration mechanism using different experimental setups, such as with and without head immobilization techniques.

As expected, we observed that the orientation of the rat head to the blast wave influenced the distribution of brain pressures. Contrary to the experimental measurements that showed higher rat brain pressures for frontal blasts when compared to lateral blasts [38], our results suggest that the frontal impact induces lower rat brain pressures than the lateral impact when measured at the coup, middle, and contre-coup regions. We postulate that the lower pressures for the frontal blast are caused by the presence of the facial components, which deflect and absorb the blast waves in the frontal blasts, whereas in the lateral blasts the waves reach the brain without significant interaction with the facial components. The difference between computational and experimental results remains to be further investigated.

There are some limitations in our study. First, we acknowledge that the 2D model cannot capture the blast wave–head interaction in its entirety. The 2D modeling approach was guided by the need to perform an exploratory investigation of the acceleration mechanisms (i.e., a comparison between the all-effects and acceleration-only models) before a detailed 3D head model can be developed. Such an approach is along the lines of the investigation of blast-induced brain cavitation using a 2D human head model [30]. Moreover, to accurately capture the spatial distribution of brain pressures, we developed a detailed rat brain model (comprising of 10 components, plus the facial bone and eye from MRI images) instead of relying on idealized geometries of the rat brain and head. Second, we used a linear viscoelastic material property for the brain tissue, which is based on a widely accepted bTBI

simulation study [27]. Use of different material models and material constants may or may not [35] change the magnitude of the predicted brain pressure. However, we expect the same relationships and patterns of brain pressure to hold even with different material models.

However, even with these limitations, the brain pressures predicted from this model were close to the experimental measurements for a rat brain. For the frontal impacts, the brain pressures ranged from 69.2 kPa to 118.0 kPa for the 100 kPa incident BOP. Experiments performed by Sundaramurthy et al. [29] reported peak intracranial pressures of 120 kPa for an incident BOP of 115 kPa. Further, the reflected pressures predicted by our model were similar to theoretical values. The model-predicted reflected pressure for a lateral impact was 271 kPa, which was close to 274.2 kPa, a theoretical calculation based on the following equation [13]:

$$\frac{\mathrm{OPRs}}{\mathrm{OPS}} = \frac{(14 \times P0) + (8 \times \mathrm{OPS})}{(7 \times P0) + \mathrm{OPS}} \tag{1}$$

where OPRs denotes the reflected pressure, OPS denotes the incident overpressure, and $P0$ represents the atmospheric pressure.

In summary, we quantitatively characterized the contribution of blast-induced head acceleration on brain pressures in rat heads using 2D computational models. The uniqueness of our model is its ability to capture the brain pressure solely from acceleration, i.e., without the contribution of skull flexure, wave propagation, or cavitation. The results from our simulations demonstrated that head acceleration, which traditionally has been overlooked in the literature, has a major effect on brain pressure, especially in regions away from the middle of the brain. Our results also demonstrated that the current practice of measuring rodent brain pressure close to the center of the brain cannot delineate the contribution of the acceleration mechanism.

Acknowledgment

This research was supported by the U.S. Army Network Science Initiative, U.S. Army Medical Research and Materiel Command, Fort Detrick, MD, the U.S. Department of Defense High Performance Computing Modernization Program, and the Defense Health Agency. The rat head MRI images were acquired at the University of Utah Small Animal Imaging Facility on an instrument funded by NIH Grant No. S10 RR23017. The opinions and assertions contained herein are the private views of the authors and do not reflect the views of the U.S. Army or of the U.S. Department of Defense.

References

[1] Tanielian, T., and Jaycox, L. H., eds., 2008, *Invisible Wounds of War: Psychological and Cognitive Injuries, Their Consequences, and Services to Assist Recovery*, Rand Corporation, Santa Monica, CA.
[2] Ritenour, A. E., Blackbourne, L. H., Kelly, J. F., McLaughlin, D. F., Pearse, L. A., Holcomb, J. B., and Wade, C. E., 2010, "Incidence of Primary Blast Injury in U.S. Military Overseas Contingency Operations: A Retrospective Study," Ann. Surg., **251**(6), pp. 1140–1144.
[3] Owens, B. D., Kragh, J. F. J., Macaitis, J., Svoboda, S. J., and Wenke, J. C., 2007, "Characterization of Extremity Wounds in Operation Iraqi Freedom and Operation Enduring Freedom," J. Orthop. Trauma, **21**(4), pp. 254–257.
[4] Bird, S. M., and Fairweather, C. B., 2007, "Military Fatality Rates (by Cause) in Afghanistan and Iraq: A Measure of Hostilities," Int. J. Epidemiol., **36**(4), pp. 841–846.
[5] Elder, G. A., and Cristian, A., 2009, "Blast-Related Mild Traumatic Brain Injury: Mechanisms of Injury and Impact on Clinical Care," Mount Sinai J. Med. (New York), **76**(2), pp. 111–118.
[6] Ling, G., Bandak, F., Armonda, R., Grant, G., and Ecklund, J., 2009, "Explosive Blast Neurotrauma," J. Neurotrauma, **26**(6), pp. 815–825.
[7] Taber, K. H., Warden, D. L., and Hurley, R. A., 2006, "Blast-Related Traumatic Brain Injury: What is Known?" J. Neuropsychiatry Clin. Neurosci., **18**(2), pp. 141–145.
[8] Taylor, P. A., and Ford, C. C., 2009, "Simulation of Blast-Induced Early-Time Intracranial Wave Physics Leading to Traumatic Brain Injury," ASME J. Biomech. Eng., **131**(6), p. 061007.
[9] Bolander, R., Mathie, B., Bir, C., Ritzel, D., and VandeVord, P., 2011, "Skull Flexure as a Contributing Factor in the Mechanism of Injury in the Rat When Exposed to a Shock Wave," Ann. Biomed. Eng., **39**(10), pp. 2550–2559.
[10] Goeller, J., Wardlaw, A., Treichler, D., O'Bruba, J., and Weiss, G., 2012, "Investigation of Cavitation as a Possible Damage Mechanism in Blast-Induced Traumatic Brain Injury," J. Neurotrauma, **29**(10), pp. 1970–1981.
[11] Panzer, M. B., Myers, B. S., and Bass, C. R., 2013, "Mesh Considerations for Finite Element Blast Modelling in Biomechanics," Comput. Methods Biomech. Biomed. Eng., **16**(6), pp. 612–621.
[12] Gullotti, D. M., Beamer, M., Panzer, M. B., Chen, Y. C., Patel, T. P., Yu, A., Jaumard, N., Winkelstein, B., Bass, C. R., Morrison, B., and Meaney, D. F., 2014, "Significant Head Accelerations Can Influence Immediate Neurological Impairments in a Murine Model of Blast-Induced Traumatic Brain Injury," ASME J. Biomech. Eng., **136**(9), p. 091004.
[13] Shridharani, J. K., Wood, G. W., Panzer, M. B., Capehart, B. P., Nyein, M. K., Radovitzky, R. A., and Bass, C. R., 2012, "Porcine Head Response to Blast," Front. Neurol., **3**, p. 70.
[14] Goldstein, L. E., Fisher, A. M., Tagge, C. A., Zhang, X. L., Velisek, L., Sullivan, J. A., Upreti, C., Kracht, J. M., Ericsson, M., Wojnarowicz, M. W., Goletiani, C. J., Maglakelidze, G. M., Casey, N., Moncaster, J. A., Minaeva, O., Moir, R. D., Nowinski, C. J., Stern, R. A., Cantu, R. C., Geiling, J., Blusztajn, J. K., Wolozin, B. L., Ikezu, T., Stein, T. D., Budson, A. E., Kowall, N. W., Chargin, D., Sharon, A., Saman, S., Hall, G. F., Moss, W. C., Cleveland, R. O., Tanzi, R. E., Stanton, P. K., and McKee, A. C., 2012, "Chronic Traumatic Encephalopathy in Blast-Exposed Military Veterans and a Blast Neurotrauma Mouse Model," Sci. Transl. Med., **4**(134), pp. 134–160.
[15] Leggieri, M. J., 2011, "Computational Modeling of Non-Impact, Blast-Induced Mild Traumatic Brain Injury (mTBI)," NATO Symposium, A Survey of Blast Injury Across the Full Landscape of Military Science, Halifax, NS.
[16] Chavko, M., Watanabe, T., Adeeb, S., Lankasky, J., Ahlers, S., and McCarron, R., 2011, "Transfer of the Pressure Wave Through the Body and Its Impact on the Brain," NATO Symposium: A Survey of Blast Injury across the Full Landscape of Military Science, Halifax, NS.
[17] Hua, Y., Kumar Akula, P., Gu, L., Berg, J., and Nelson, C. A., 2014, "Experimental and Numerical Investigation of the Mechanism of Blast Wave Transmission Through a Surrogate Head," J. Comput. Nonlinear Dyn., **9**(3), p. 031010.
[18] Ganpule, S., Alai, A., Plougonven, E., and Chandra, N., 2013, "Mechanics of Blast Loading on the Head Models in the Study of Traumatic Brain Injury Using Experimental and Computational Approaches," Biomech. Model. Mechanobiol., **12**(3), pp. 511–531.
[19] Skotak, M., Wang, F., Alai, A., Holmberg, A., Harris, S., Switzer, R. C., and Chandra, N., 2013, "Rat Injury Model Under Controlled Field-Relevant Primary Blast Conditions: Acute Response to a Wide Range of Peak Overpressures," J. Neurotrauma, **30**(13), pp. 1147–1160.
[20] Long, J. B., Bentley, T. L., Wessner, K. A., Cerone, C., Sweeney, S., and Bauman, R. A., 2009, "Blast Overpressure in Rats: Recreating a Battlefield Injury in the Laboratory," J. Neurotrauma, **26**(6), pp. 827–840.
[21] Meaney, D. F., Morrison, B., and Dale Bass, C., 2014, "The Mechanics of Traumatic Brain Injury: A Review of What We Know and What We Need to Know for Reducing Its Societal Burden," ASME J. Biomech. Eng., **136**(2), p. 021008.
[22] Morrison, B., III, Elkin, B. S., Dollé, J. P., and Yarmush, M. L., 2011, "In Vitro Models of Traumatic Brain Injury," Annu. Rev. Biomed. Eng., **13**(1), pp. 91–126.
[23] Johnson, G. A., Calabrese, E., Badea, A., Paxinos, G., and Watson, C., 2012, "A Multidimensional Magnetic Resonance Histology Atlas of the Wistar Rat Brain," NeuroImage, **62**(3), pp. 1848–1856.
[24] Abdullah, O., and Hsu, E., 2014, Personal Communication.
[25] Bailey, S. A., Zidell, R. H., and Perry, R. W., 2004, "Relationships Between Organ Weight and Body/Brain Weight in the Rat: What is the Best Analytical Endpoint?" Toxicol. Pathol., **32**(4), pp. 448–466.
[26] Mao, H., Jin, X., Zhang, L., Yang, K. H., Igarashi, T., Noble-Haeusslein, L. J., and King, A. I., 2010, "Finite Element Analysis of Controlled Cortical Impact-Induced Cell Loss," J. Neurotrauma, **27**(5), pp. 877–888.
[27] Zhu, F., Mao, H., Dal Cengio Leonardi, A., Wagner, C., Chou, C., Jin, X., Bir, C., Vandevord, P., Yang, K. H., and King, A. I., 2010, "Development of an FE Model of the Rat Head Subjected to Air Shock Loading," Stapp Car Crash J., **54**, pp. 211–225.
[28] Mao, H., Wagner, C., Guan, F., Yeni, Y. N., and Yang, K. H., 2011, "Material Properties of adult Rat Skull," J. Mech. Med. Biol., **11**(5), pp. 1199–1212.
[29] Sundaramurthy, A., Alai, A., Ganpule, S., Holmberg, A., Plougonven, E., and Chandra, N., 2012, "Blast-Induced Biomechanical Loading of the Rat: An Experimental and Anatomically Accurate Computational Blast Injury Model," J. Neurotrauma, **29**(13), pp. 2352–2364.
[30] Panzer, M. B., Myers, B. S., Capehart, B. P., and Bass, C. R., 2012, "Development of a Finite Element Model for Blast Brain Injury and the Effects of CSF Cavitation," Ann. Biomed. Eng., **40**(7), pp. 1530–1544.
[31] Mao, H., Zhang, L., Jiang, B., Genthikatti, V. V., Jin, X., Zhu, F., Makwana, R., Gill, A., Jandir, G., Singh, A., and Yang, K. H., 2013, "Development of a Finite Element Human Head Model Partially Validated With Thirty Five Experimental Cases," ASME J. Biomech. Eng., **135**(11), p. 111002.
[32] Takhounts, E. G., Ridella, S. A., Hasija, V., Tannous, R. E., Campbell, J. Q., Malone, D., Danelson, K., Stitzel, J., Rowson, S., and Duma, S., 2008, "Investigation of Traumatic Brain Injuries Using the Next Generation of Simulated Injury Monitor (SIMon) Finite Element Head Model," Stapp Car Crash J., **52**, pp. 1–31.
[33] Zhang, L., Yang, K. H., Dwarampudi, R., Omori, K., Li, T., Chang, K., Hardy, W. N., Khalil, T. B., and King, A. I., 2001, "Recent Advances in Brain Injury Research: A New Human Head Model Development and Validation," Stapp Car Crash J., **45**, pp. 369–394.

[34] Zhao, W., Ruan, S., and Ji, S., 2015, "Brain Pressure Responses in Translational Head Impact: A Dimensional Analysis and a Further Computational Study," Biomech. Model. Mechanobiol., **14**(4), pp. 753–766.
[35] Singh, D., Cronin, D. S., and Haladuick, T. N., 2014, "Head and Brain Response to Blast Using Sagittal and Transverse Finite Element Models," Int. J. Numer. Methods Biomed. Eng., **30**(4), pp. 470–489.
[36] Effgen, G. B., Hue, C. D., Vogel, E., 3rd, Panzer, M. B., Meaney, D. F., Bass, C. R., and Morrison, B., III, 2012, "A Multiscale Approach to Blast Neurotrauma Modeling: Part II: Methodology for Inducing Blast Injury to In Vitro Models," Front. Neurol., **3**, p. 23.
[37] Yeoh, S., Bell, E. D., and Monson, K. L., 2013, "Distribution of Blood-Brain Barrier Disruption in Primary Blast Injury," Ann. Biomed. Eng., **41**(10), pp. 2206–2214.
[38] Chavko, M., Watanabe, T., Adeeb, S., Lankasky, J., Ahlers, S. T., and McCarron, R. M., 2011, "Relationship Between Orientation to a Blast and Pressure Wave Propagation Inside the Rat Brain," J. Neurosci. Methods, **195**(1), pp. 61–66.
[39] Leonardi, A. D., Bir, C. A., Ritzel, D. V., and VandeVord, P. J., 2011, "Intracranial Pressure Increases During Exposure to a Shock Wave," J. Neurotrauma, **28**(1), pp. 85–94.